Supplemental Material

Journal of Climate
Ocean–Land Teleconnections and Chaotic Atmospheric Variability
https://doi.org/10.1175/JCLI-D-23-0740.1

Supplementary Material for

Ocean-Land Teleconnections and Chaotic Atmospheric Variability

Randal D. Koster[1], Siegfried D. Schubert[1,2], Anthony M. DeAngelis[1,2],
Yehui Chang[1,3], and Adam A. Scaife[4,5]

[1]*Global Modeling and Assimilation Office, NASA/Goddard Space Flight Center, Greenbelt, MD USA*

[2]*Science Systems and Applications, Inc., Lanham, MD, USA*

[3]*Morgan State University, Baltimore, Maryland, USA*

[4]*Met Office Hadley Centre, Met Office, Fitz Roy Road, Exeter, Devon, UK*

[5]*Department of Mathematics and Statistics, University of Exeter, UK*

S.1 Derivation of Equations in Text

We start by deriving (12) in the main text [the equation for $\mathrm{Corr}^2(Y_o,Y_m)$], given that (3) [the corresponding equation for $\mathrm{Corr}^2(Y_{mn},Y_m)$] follows immediately from it. From (1), (2), and (11) in the main text, we have

$$Y_{mn}(t) = B_m(t) + \varepsilon_{mn}(t), \tag{S1}$$

$$Y_m(t) = \frac{1}{N}\sum_1^N Y_{mn}(t). \tag{S2}$$

and

$$Y_o(t) = B_o(t) + \varepsilon_o(t). \tag{S3}$$

Removing the "(t)" for notational simplicity, we can compute

$$\mathrm{Corr}^2(Y_o,Y_m) = \frac{\mathrm{Cov}^2(Y_o,Y_m)}{\sigma_{Y_o}^2\,\sigma_{Y_m}^2} \tag{S4}$$

$$= \frac{\overline{(B_o+\varepsilon_o)\left(\frac{1}{N}\sum_1^N(B_m(t)+\varepsilon_{mn})\right)}^2}{\sigma_{Y_o}^2\sigma_{Y_m}^2} \tag{S5}$$

where the overbar refers to a time mean. Because the ε terms are completely noncorrelated with everything else, this simplifies to

$$\mathrm{Corr}^2(Y_o,Y_m) = \frac{\mathrm{Cov}^2(B_o,B_m)}{\sigma_{Y_o}^2\sigma_{Y_m}^2} \tag{S6}$$

$$= \frac{\mathrm{Corr}^2(B_o,B_m)\sigma_{B_o}^2\sigma_{B_m}^2}{\sigma_{Y_o}^2\sigma_{Y_m}^2} \tag{S7}$$

Now compute the variance of both sides of (S3), making use again of the fact that B_o and ε_o are uncorrelated:

$$\sigma_{Y_o}^2 = \sigma_{B_o}^2 + \sigma_{\varepsilon_o}^2 \tag{S8}$$

Similarly, from (S1),

$$\sigma_{Y_{mn}}^2 = \sigma_{B_m}^2 + \sigma_{\varepsilon_{mn}}^2 \tag{S9}$$

and considering (S2), we get

$$\sigma_{Y_m}^2 = \sigma_{B_m}^2 + {}^{\sigma_{\varepsilon_{mn}}^2}/_{N} \quad \text{(S10)}$$

We now define ρ^2 as the fraction of the total variance of Y stemming from the signal B:

$$\rho_o{}^2 = \frac{\sigma_{B_o}^2}{\sigma_{B_o}^2+\sigma_{\varepsilon_o}^2} \quad \text{(S11)}$$

$$\rho_m{}^2 = \frac{\sigma_{B_m}^2}{\sigma_{B_m}^2+\sigma_{\varepsilon_{mn}}^2} \quad \text{(S12)}$$

noting along the way that

$$\rho_o{}^2 = Corr^2(Y_o, B_o) \quad \text{(S13)}$$

$$\rho_m{}^2 = Corr^2(Y_{mn}, B_m) \quad \text{(S14)}$$

Incorporating (S8), (S10), and (S11) into (S7) gives

$$\mathrm{Corr}^2(Y_o, Y_m) = \frac{\rho_o^2\ \mathrm{Corr}^2(B_o,B_m)\sigma_{B_m}^2}{\sigma_{B_m}^2+{}^{\sigma_{\varepsilon_{mn}}^2}/_{N}} \quad \text{(S15)}$$

Noting that (S12) can be arranged to give

$$\sigma_{\varepsilon_{mn}}^2 = \frac{1-\rho_m^2}{\rho_m^2}\ \sigma_{B_m}^2, \quad \text{(S16)}$$

we get equation (12) in the text:

$$\mathrm{Corr}^2(Y_o\ , Y_m\ ) = \frac{\rho_o^2\mathrm{Corr}^2(B_o,B_m)}{\left(1+\frac{[1-\rho_m^2]/\rho_m^2}{N}\right)} \quad \text{(S17)}$$

The derivation of Equation (3) in the text is identical except for a notable simplification. Because $\mathrm{Corr}^2(B_m,B_m)$ is identically 1, and because we are dealing with model quantities ($\rho_m{}^2$) rather than observational quantities ($\rho_o{}^2$), we get

$$\mathrm{Corr}^2(Y_{mn}, Y_m) = \frac{\rho_m^2}{\left(1+\frac{[1-\rho_m^2]/\rho_m^2}{N}\right)} \tag{S18}$$

Now, for the derivation of equation (10) in the text, we write (in analogy to (S7)):

$$\mathrm{Corr}^2(Y_m, Y_q) = \frac{\mathrm{Corr}^2(B_m, B_q)\,\sigma_{Bm}^2\,\sigma_{Bq}^2}{\sigma_{Ym}^2\sigma_{Yq}^2} \tag{S19}$$

$$= \frac{\mathrm{Corr}^2(B_m, B_q)\,\sigma_{Bm}^2\,\sigma_{Bq}^2}{\left[\sigma_{Bm}^2 + {\sigma_{\varepsilon mn}^2}/{N}\right]\left[\sigma_{Bq}^2 + {\sigma_{\varepsilon qn}^2}/{N_q}\right]} \tag{S20}$$

Using (S16) and the analogous equation for model q gives, upon rearrangement, Equation (10) in the main text.

S.2 Analysis of the Reliability of the $Corr^2(B_o,B_m)$ Calculations

If AGCMs share common deficiencies that lead to dependent errors – that is, if models tend to look more like each other than they look like the real world – then our estimates of $Corr^2(B_m,B_q)$ will be significantly different (presumably higher) than our target, an estimate for $Corr^2(B_o,B_m)$. To examine this, we compute the JJA correlations between the GEOS ensemble mean monthly T2M time series and the observations as well as that between the GEOS ensemble mean monthly time series and a single simulation from each of the AGCMs listed in Table 1 of the main text. We consider single simulations of these other AGCMs to put the observations and these other AGCM results on the same footing – for this particular comparison, we do not want to obtain higher correlations with these other AMIP models simply through the averaging out of their within-model (intra-ensemble) noise.

Figure S1 shows the results. If the GEOS model tended to look more like the other AGCMs than observations due to some shared model deficiency, the correlations in the first five panels should look higher than those in the last panel. Visual inspection, as well as the listed global averages, shows this not to be the case.

Consideration of alternative individual simulations from the CMIP6 models produces similar results (not shown). Indeed, when the global average correlation for each simulation is subsequently averaged over all ten simulations of that model's ensemble, we get averages of 0.208, 0.241, 0.236, 0.228, and 0.228 for the MIROC6, CESM2, NorCPM1, ACCESS, and IPSL models, respectively – similar to, and indeed slightly less than, the value of 0.235 for the observations.

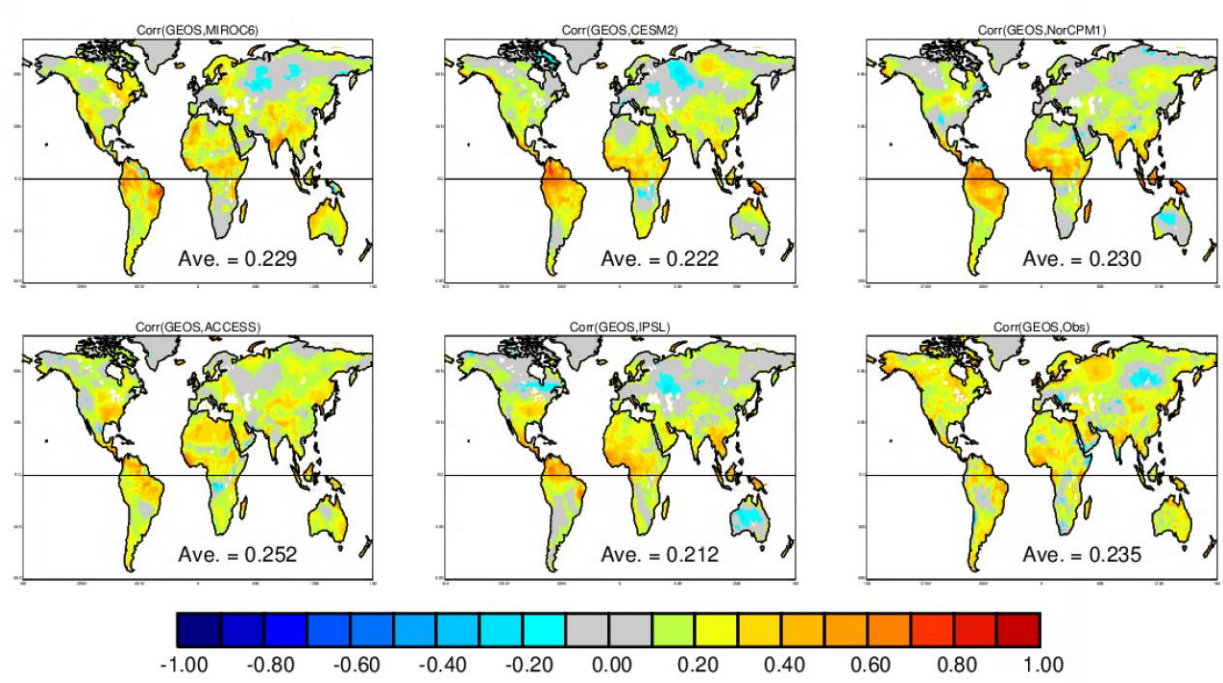

Figure S1. First five panels: Correlation between the GEOS model ensemble mean time series and the time series from individual AMIP simulations produced with the various CMIP6 models (see plot headings). Final panel: Correlation between the GEOS model ensemble mean time series and the observations.

S.3 Demonstration that Ten Ensemble Members Provides Reasonable Estimates of ρ_m^2

Key to our extraction of ρ_m^2 is our ability to fit Equation (3) to data produced by the AGCM ensemble, along the lines of what was demonstrated in Figure 1 of the main text:

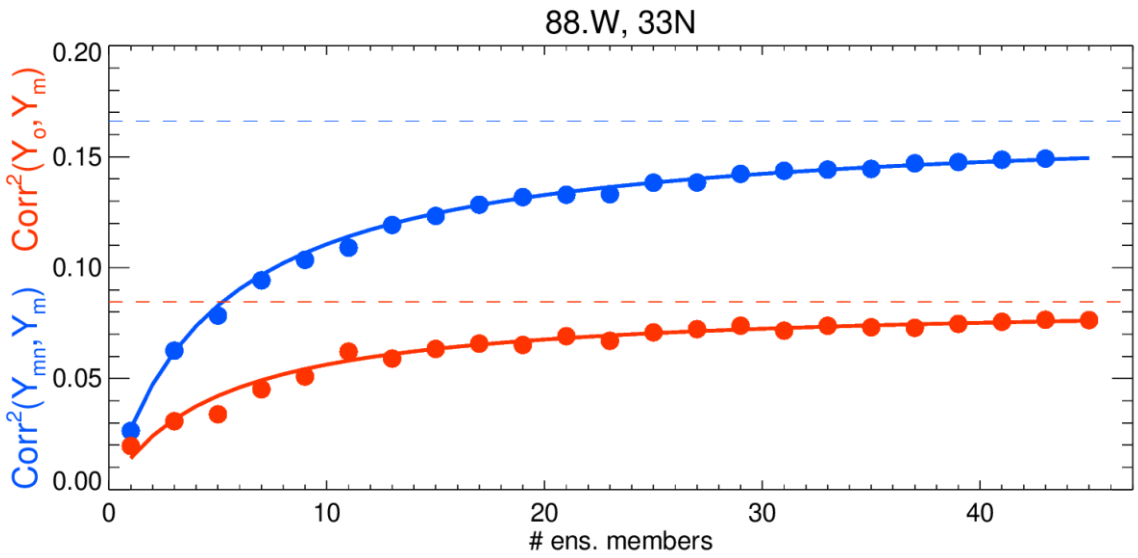

Figure S2. Repeat of Figure 1 in the main text: Representative examples of how key model relationships vary with ensemble size, focusing on the simulation of monthly mean air temperature, T2M. Blue dots: variation of $Corr^2(Y_{mn},Y_m)$ with ensemble size, where $Corr^2(Y_{mn},Y_m)$ characterizes the ability of the ensemble mean to capture the variability produced by a single ensemble member. Red dots: variation of $Corr^2(Y_o,Y_m)$ with ensemble size, where $Corr^2(Y_o,Y_m)$ characterizes the ability of the ensemble mean to capture the variability seen in the observations. The lines through the dots are determined through a fitting procedure, which provides as a matter of course the indicated asymptotes, shown as dashed lines (see text). Results shown are for JJA.

For the blue dots, our algorithm searches for the single value of ρ_m^2 that produces the best fit through the dots; this value of ρ_m^2 also serves as the asymptote for the plotted blue relationship. The potential for using 44 dots to define the curve (22 are used here for computational tractability) allows for substantial robustness in the ρ_m^2 estimation. In dealing with the CMIP models, however, we must address an important issue: with only ten ensemble members, a maximum of nine dots can be used to estimate ρ_m^2 (or ρ_q^2, to use our earlier CMIP-specific terminology). Is this adequate for the fitting of the curve and the determination of the asymptotic ρ_m^2?

While we cannot address this directly with the CMIP data themselves, we can do the next best thing: we can determine quantitatively how well we can reproduce the asymptotes already found using the full 45-member GEOS ensemble if we instead draw our ensemble subsets from only the first 10 members of the GEOS ensemble. Such an exercise is akin to fitting the curve through the first five dots in Figure S2, though the potential for noise is stronger here, given that the source of the subsetting is smaller. (Note that we could in principle use 9 dots in this exercise, corresponding to 1-9 ensemble members; we use only 5 here for computational tractability.)

Figure S3 shows a representative calculation. Even drawing from only 10 ensemble members, we are able to reproduce the value obtained with the much larger ensemble.

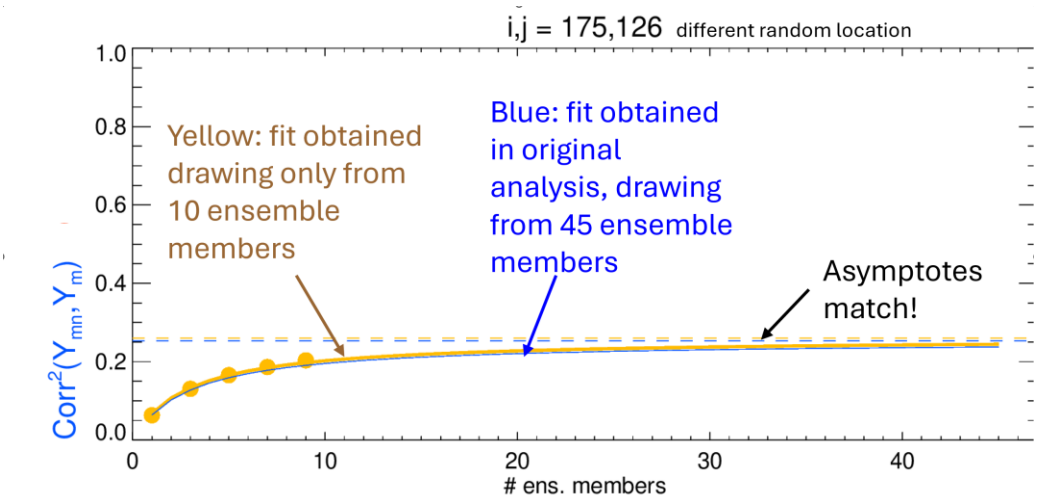

Figure S3. Demonstration that fitting the curve and thereby determining the asymptote (i.e., ρ_m^2) using only 5 dots (and subsetting from only 10 GEOS ensemble members) provides essentially the same answer as drawing from the full 45-member GEOS ensemble, which used 22 dots for the calculation (as in Figure S2).

This level of agreement indeed turns out to be typical but does not occur everywhere. Figure S4 shows an example of a poorer fit using only ten ensemble members.

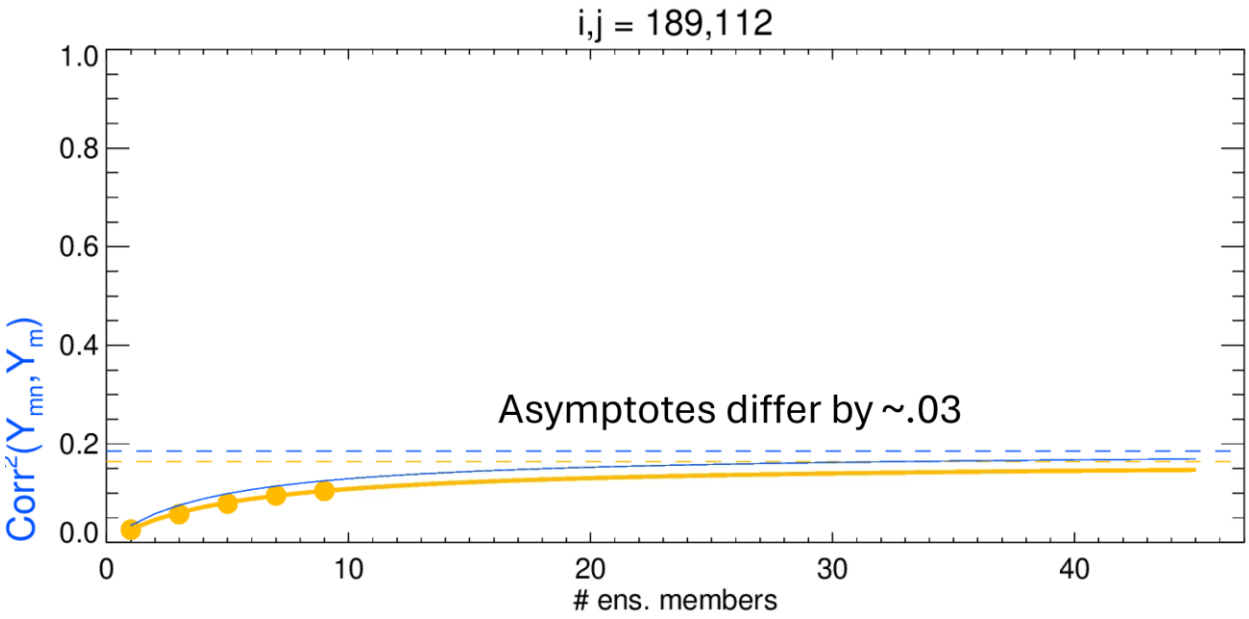

Figure S4. As in Figure S3, but at a location for which the fit is not as good.

An overall characterization of the results is provided in Figures S5-S8, which include maps showing the differences obtained in the ρ_m^2 values (those obtained drawing from 10 ensemble members minus those obtained drawing from 45 ensemble members) for the different seasons. Differences in the ρ_m^2 estimations are seen to be small across the globe and in all seasons (with typical maxima of order 0.03, as represented by the location and season examined in Figure S4), with no particular propensity for positive or negative differences.

Although these results do not constitute absolute proof, we offer them as strong support for the idea that we can extract reasonable ρ_m^2 values (i.e., ρ_q^2 values) from the 10-member CMIP ensembles.

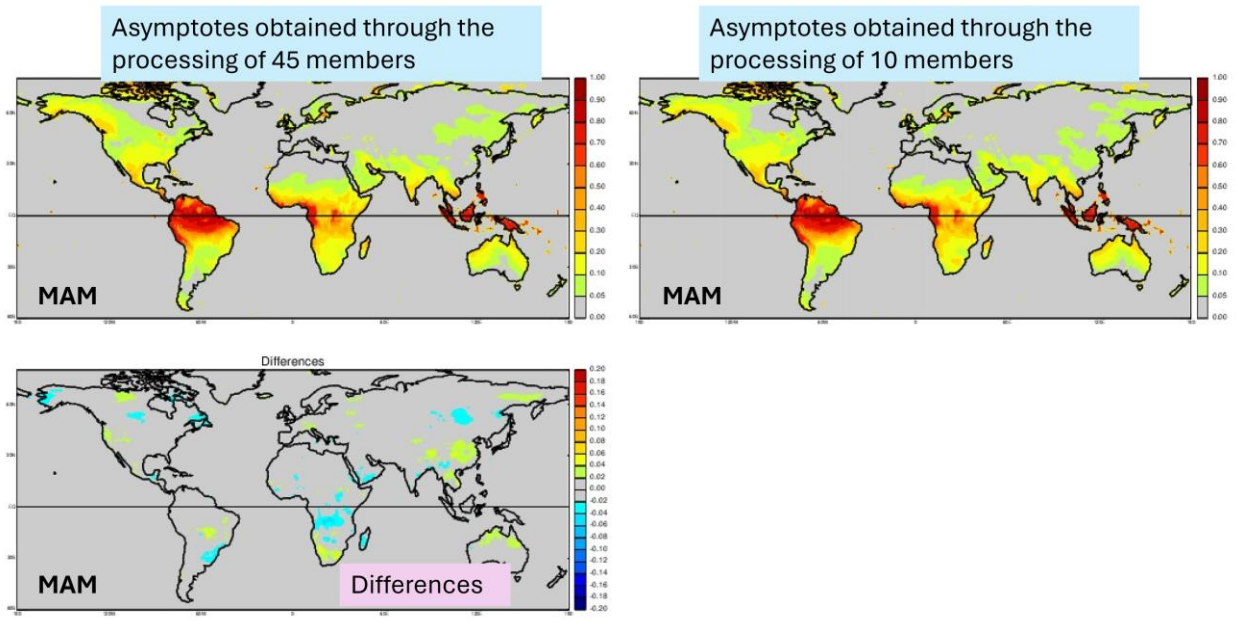

Figure S5. Top left: Values of ρ_m^2 obtained by processing data from the full 45-member GEOS ensemble, for MAM. Top right: Corresponding values of ρ_m^2 obtained by processing data from a 10-member subset of the GEOS ensemble. Bottom left: Differences (top right minus top left).

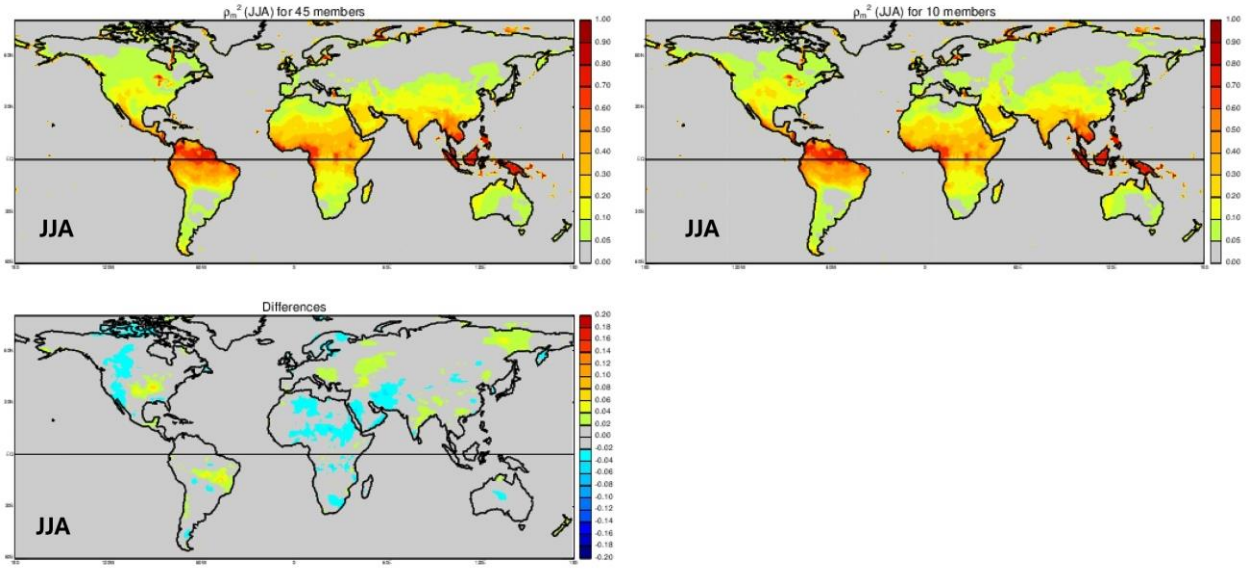

Figure S6. As in Figure S5, but for JJA.

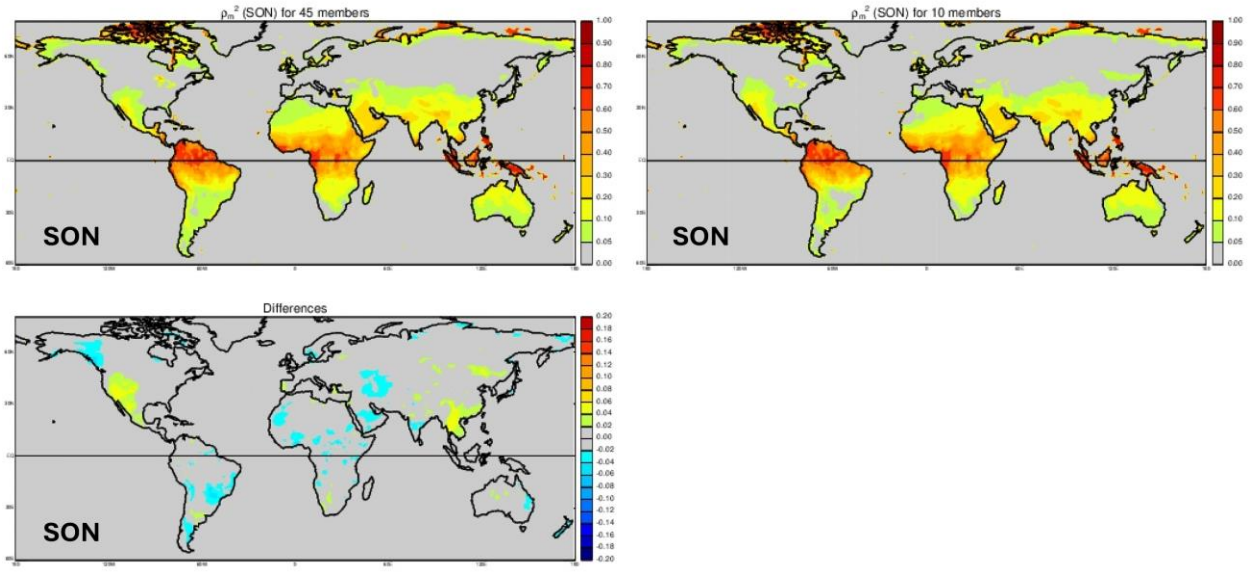

Figure S7. As in Figure S5, but for SON.

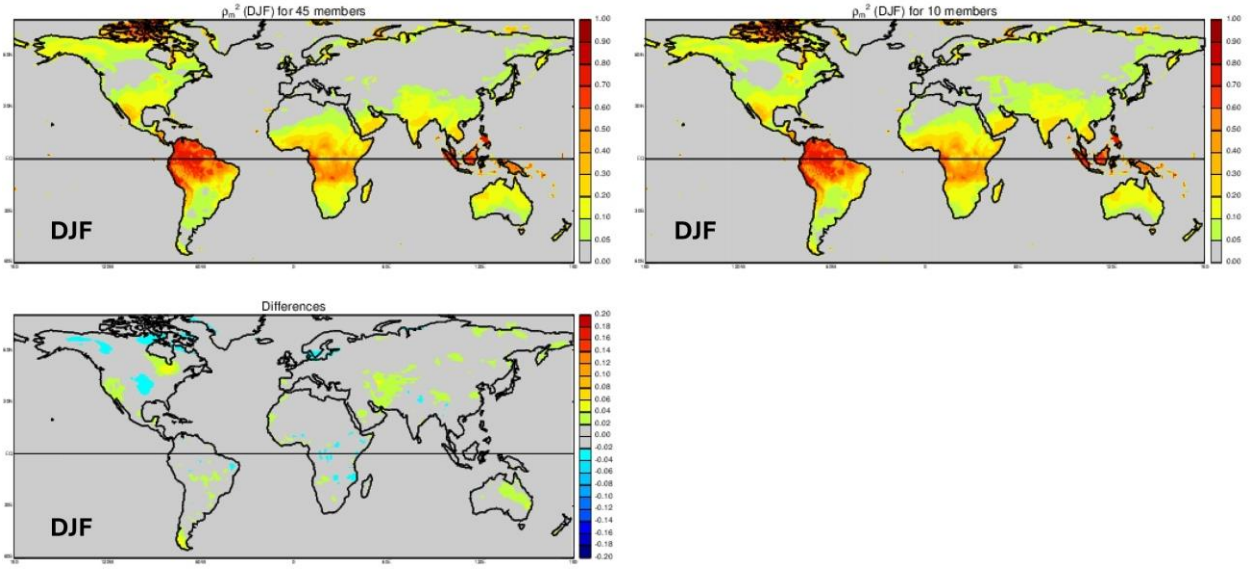

Figure S8. As in Figure S5, but for DJF.

S.4 CMIP Results for Additional Seasons

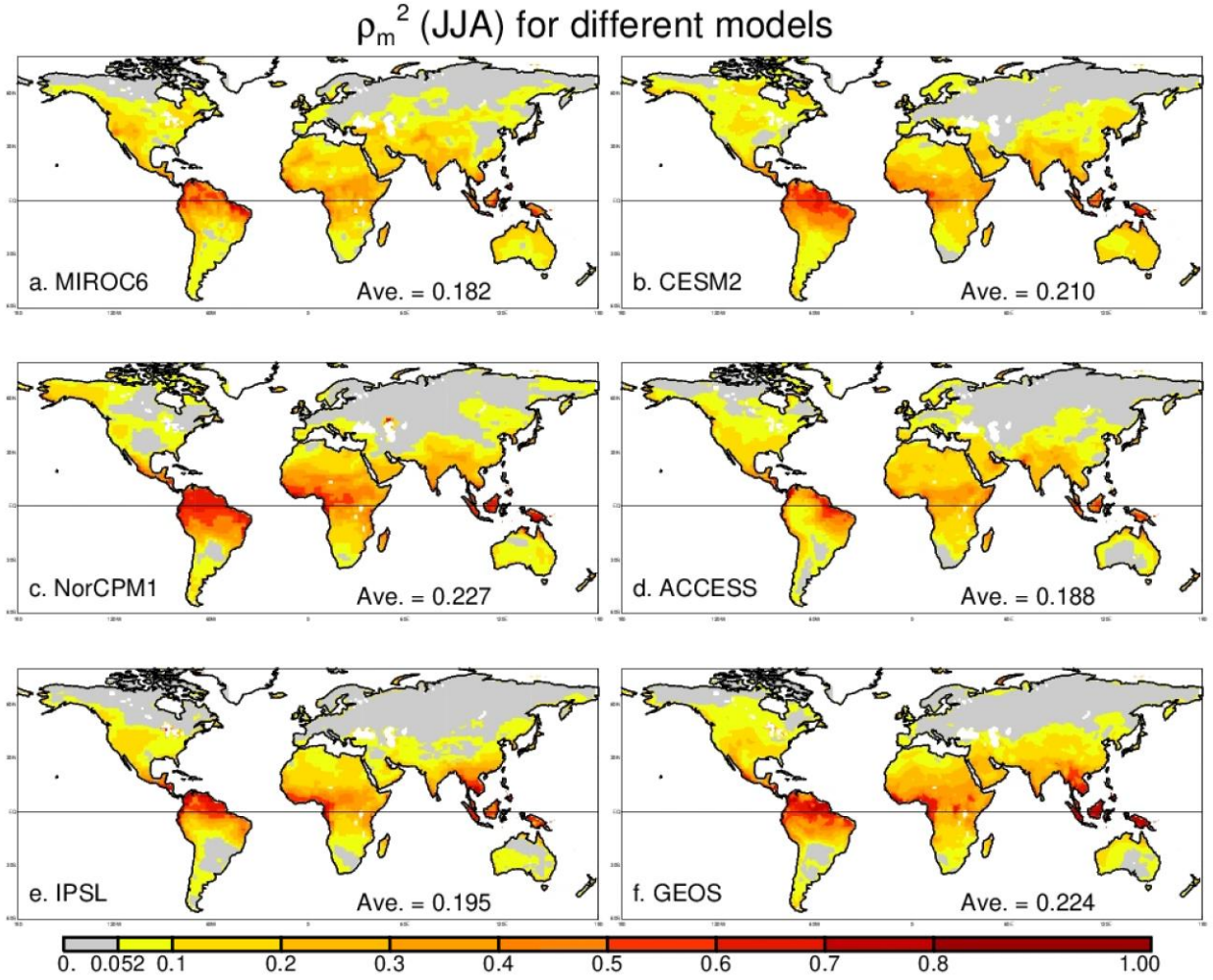

Figure S9. As in Figure 3 of the main text, but for JJA.

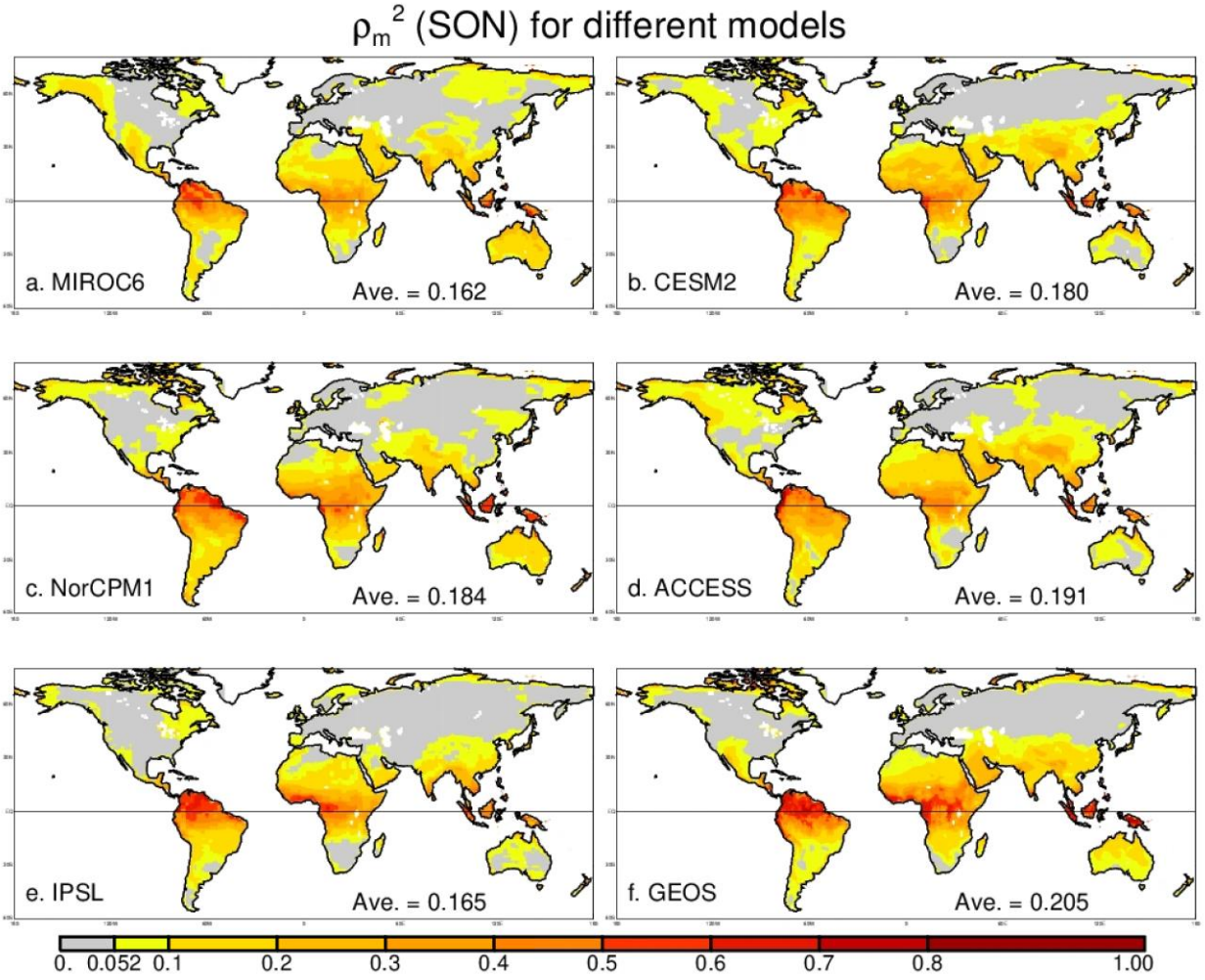

Figure S10. As in Figure 3 of the main text, but for SON.

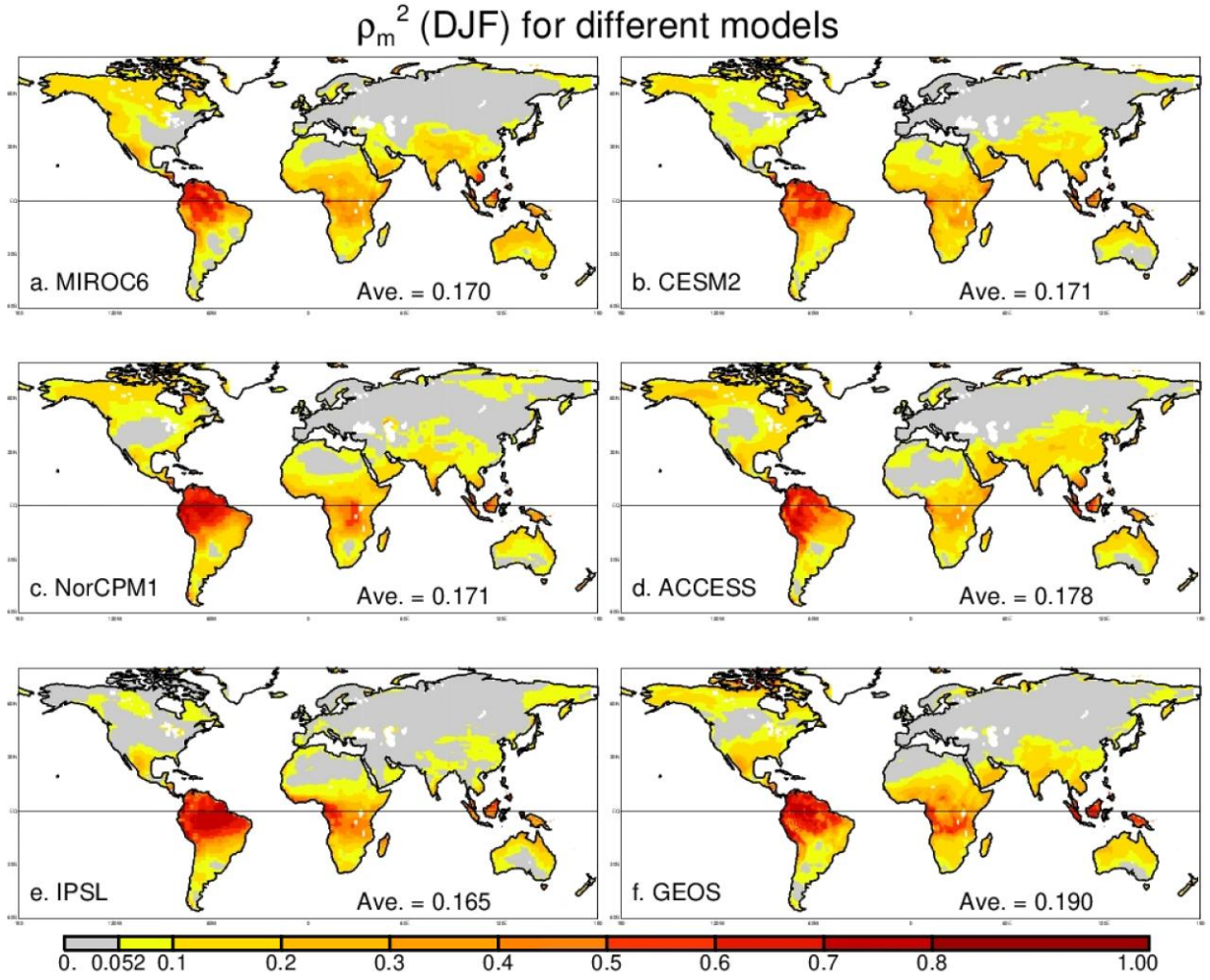

Figure S11. As in Figure 3 of the main text, but for DJF.

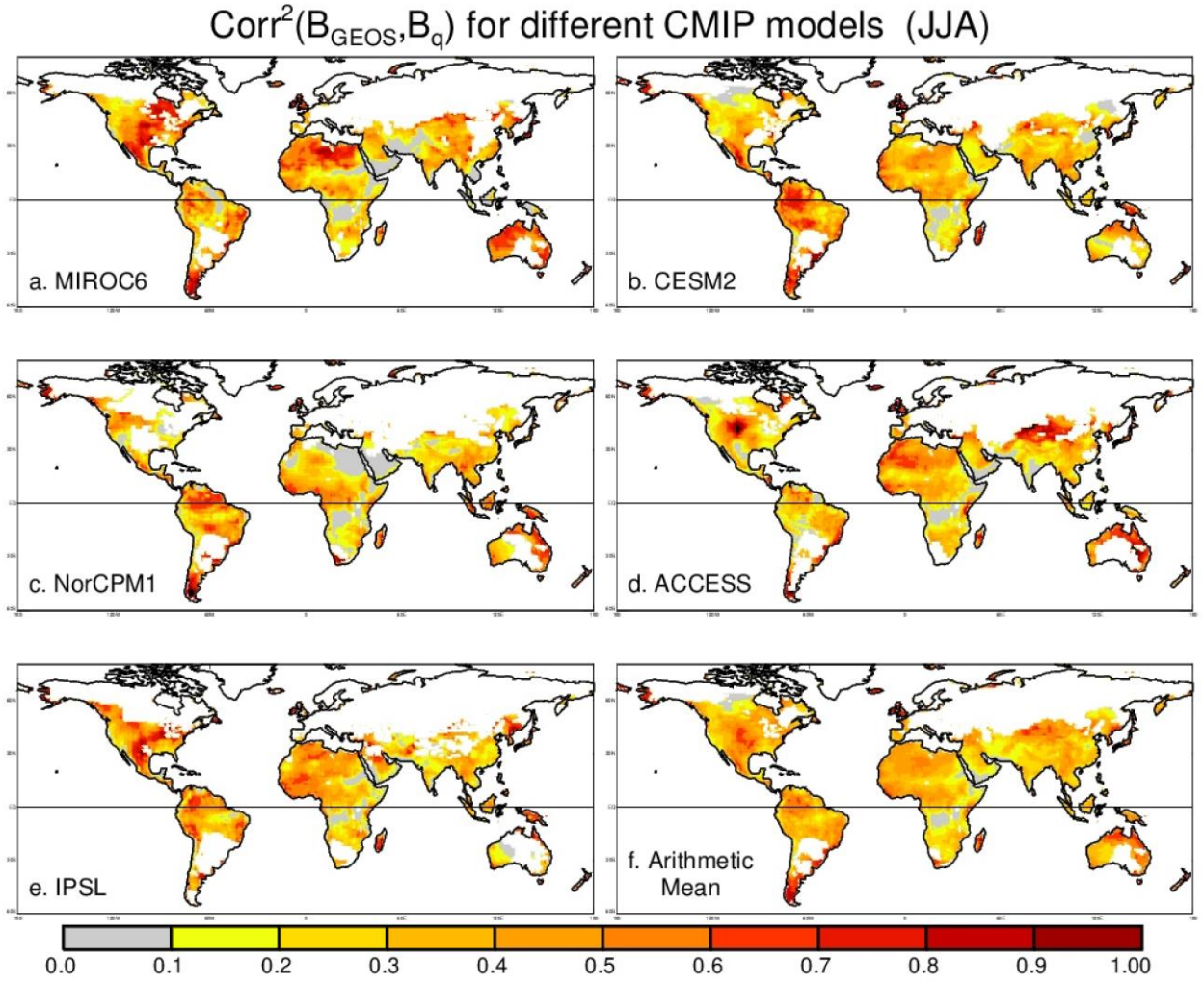

Figure S12. As in Figure 4 of the main text, but for JJA.

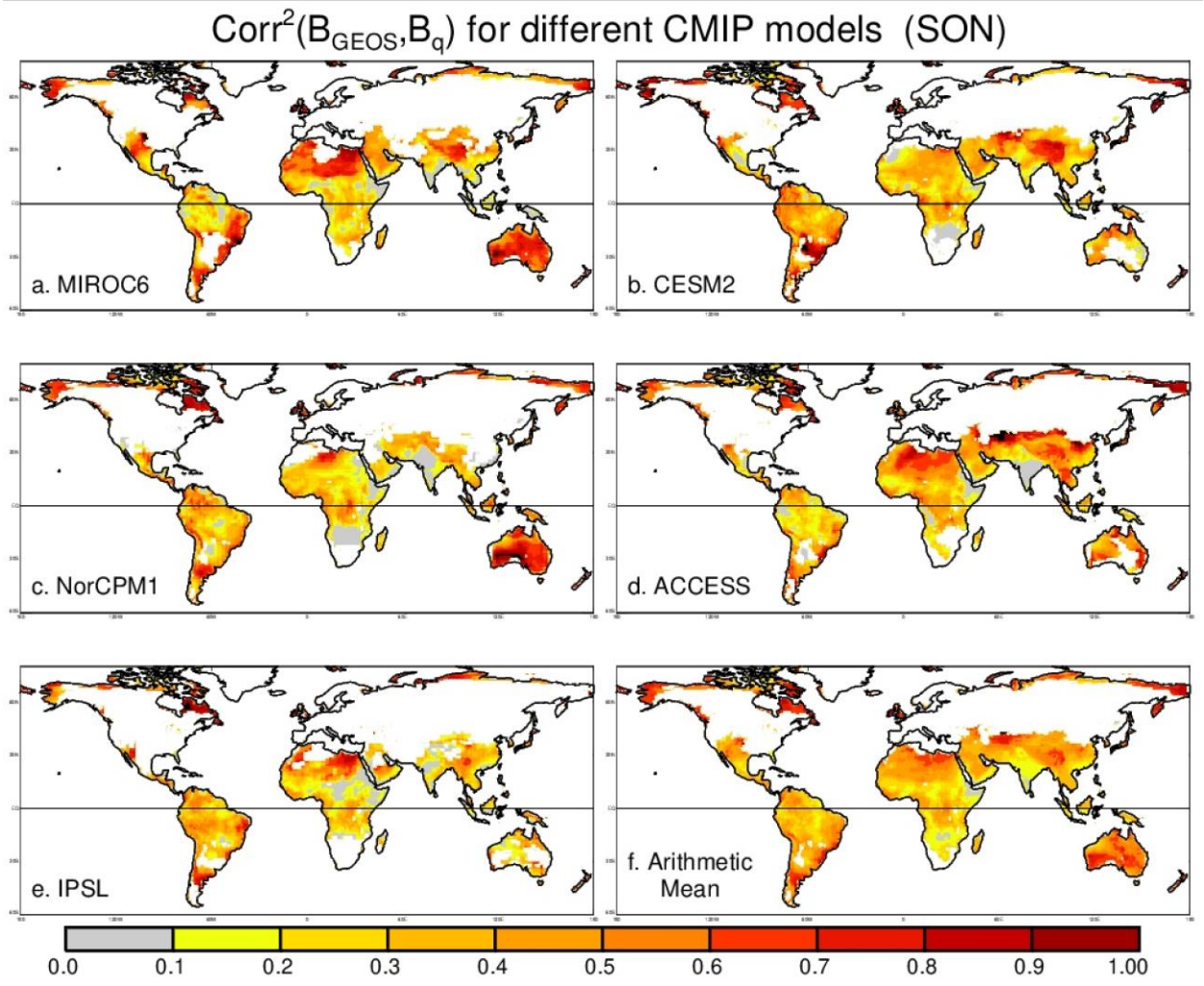

Figure S13. As in Figure 4 of the main text, but for SON.

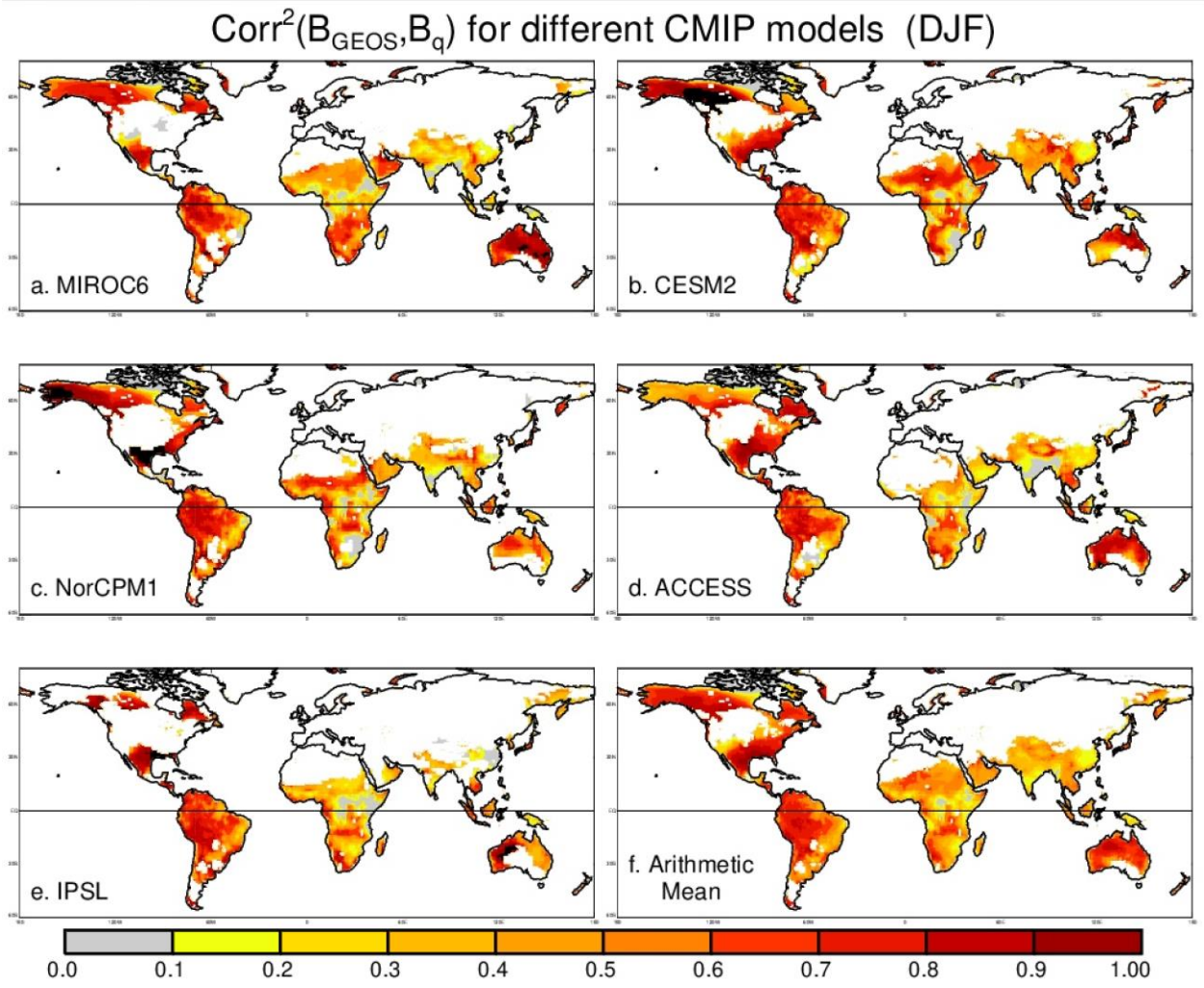

Figure S14. As in Figure 4 of the main text, but for DJF.

S.5 Estimates of Upper and Lower Bounds for ρ_o^2 for Additional Seasons

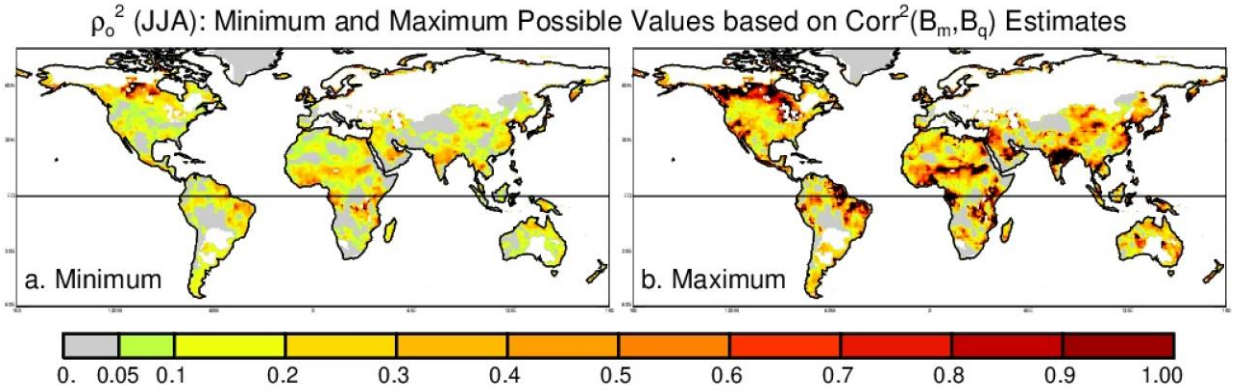

Figure S15. As in Figure 9 of the main text, but for JJA.

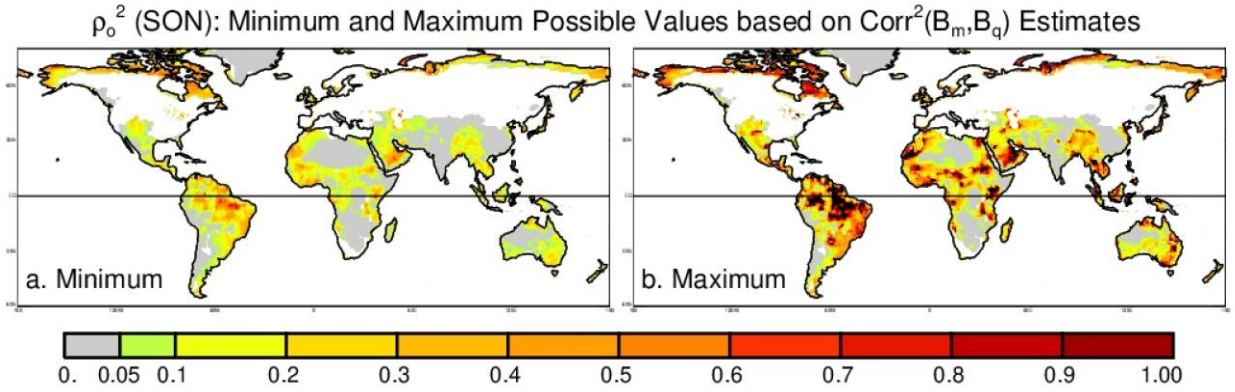

Figure S16. As in Figure 9 of the main text, but for SON.

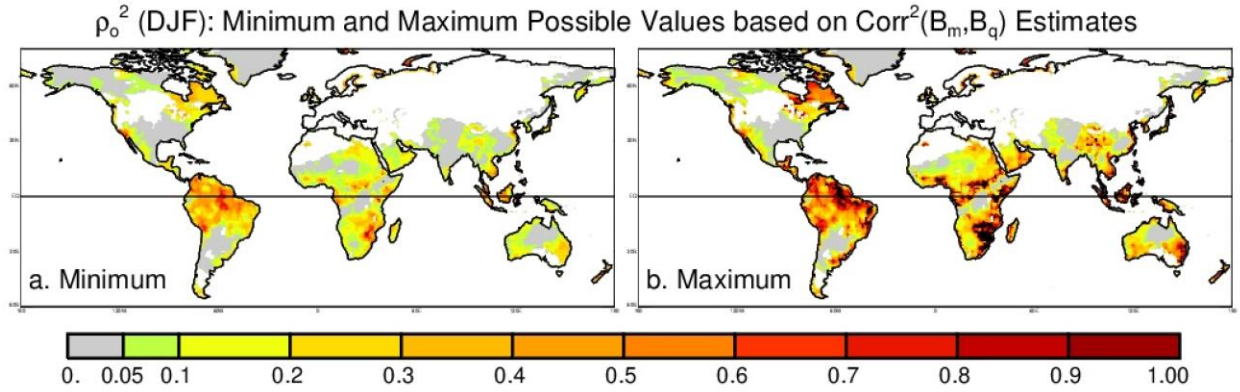

Figure S17. As in Figure 9 of the main text, but for DJF.